BULLETIN OF CANADIAN PETROLEUM GEOLOGY
VOL. 50, NO. 1 (MARCH, 2002), P. 105-117

Sedimentology and reservoir characteristics of a Middle Jurassic fluvial system, Datong Basin, Northern China

X. YU AND X. MA
Department of Energy Resources
China University of Geosciences
Beijing, China 100083

H. QING
Department of Geology
University of Regina
Regina, SK S4S 0A2

ABSTRACT

An outcrop of the Middle Jurassic Yungang Formation in Datong Basin of northern China was studied in order to provide a better understanding of the architecture and heterogeneity of hydrocarbon reservoirs associated with braided-fluvial deposits. The main section of outcrop, which is continuously exposed over 350 m, is interpreted to have been deposited in the middle-stream reaches of a sandy braided river in a proximal area at the eastern edge of the basin. Seventeen lithofacies were identified, based on petrology and sedimentary structures. These lithofacies were grouped into seven architectural elements, including channel fill, transverse bar, longitudinal bar, diagonal bar, abandoned channel fill, levee, and overbank fines. These sediments were deposited in three stages: active, abandonment, and reactivation. These reflect channel switching and waxing and waning of the fluvial system. The sandstones are mainly arkoses or lithic arkoses, with high matrix content, low compositional and textural maturity, and a variety of cements. A total of 282 specimens were collected from outcrops and analyzed for porosity and permeability. The results show that sandstones from longitudinal bar and channel fills have the highest porosity and permeability while abandoned channels and levee sediments have the lowest. In cross-section, porosity and permeability are generally highest in the middle of the sand bodies, reflecting the spatial distribution of architectural elements and petrophysical properties.

RÉSUMÉ

Un affleurement de la Formation de Yungang du Jurassique moyen du bassin de Datong du nord de la Chine a été étudié pour fournir une meilleure compréhension de l'architecture et de l'hétérogénéité des réservoirs associés aux dépôts anastomosés fluviaux. La principale coupe de l'affleurement, qui est exposée de façon continue sur plus de 350 m, est interprétée comme ayant été mise en place dans les parties médianes d'une rivière sableuse dans une région proximale à la bordure Est du bassin. Dix-sept lithofaciès sont identifiés sur la base de la pétrologie et des structures sédimentaires. Ces lithofaciès sont groupés en sept éléments architecturaux, incluant les sédiments de remplissage de barrière transversale, de barrière diagonale, de remplissage de chenal abandonné et de sédiments de levées et de sédiments fins d'inondation. Ces sédiments se sont mis en place en trois étapes : active, d'abandon et de réactivation. Celles-ci reflètent le changement, la croissance et la décroissance des chenaux du système fluvial. Les grès sont principalement des arkoses et des arkoses lithiques, avec une grande quantité de matrice, une basse maturité de composition et de texture et une diversité de ciments. Un total de 282 échantillons a été amassé des affleurements et analysés pour déterminer la porosité et la perméabilité. Les résultats montrent que les grès provenant des barrières longitudinales et des remplissages de chenaux ont la plus haute porosité et perméabilité alors que les chenaux abandonnés et les sédiments de levées ont la plus basse. En coupe, la porosité et la perméabilité sont généralement les plus élevées dans le centre des masses de grès et reflètent la distribution spatiale des éléments architecturaux et des propriétés pétrophysiques.

Traduit par Lynn Gagnon

Introduction

A significant number of oil fields in the eastern part of China are hosted in Jurassic, Cretaceous, and Tertiary terrestrial clastic sandstones. Although these rocks were deposited in a wide spectrum of sedimentary environments, fluvial and deltaic sandstones are the most important reservoirs in these fields (e.g. Qiu, 1992; Yu et al., 1994). The majority of the oil fields are currently in either secondary or tertiary recovery stages. A better understanding of the architecture and heterogeneity of these hydrocarbon reservoirs is required in order to design and implement enhanced recovery techniques.

Datong Basin is a Jurassic terrestrial basin with a fluvial and lacustrine-deltaic sedimentary infill (Fig. 1). The stratigraphic age and sedimentary environments of these rocks are similar to the petroleum reservoirs in eastern China. In order to provide a better understanding of the architecture and heterogeneity of fluvial reservoirs, we investigated the sedimentology, lithofacies, and reservoir architectures of Middle Jurassic fluvial deposits in outcrops of the Datong Basin. The Yungang outcrops near Datong City were selected for this purpose because of their extensive and continuous exposure.

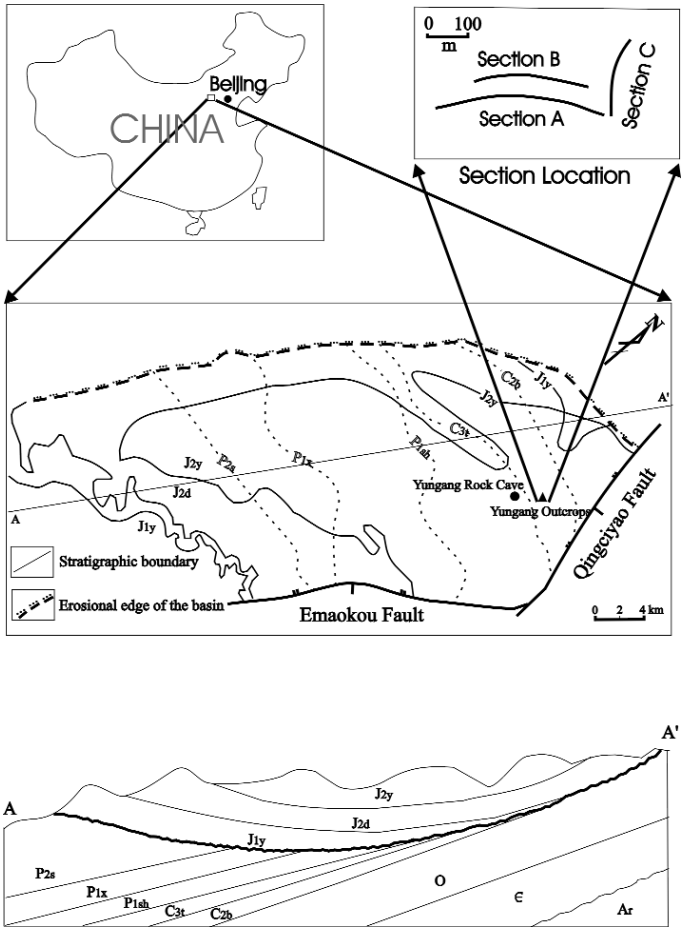

Fig. 1. Schematic diagram of the Datong Basin, Northern China, with studied outcrops. J_{2y}: Middle Jurassic Yungang Formation, the focus of this investigation. J_{1y}: Lower Jurassic Yongdingzhuang Formation; J_{2d}: Middle Jurassic Datong and Yungang formations; P_{2sh}: Upper Permian Shihezi Formation; P_{1x}: Lower Permian Shihezi Formation; P_{1s}: Lower Permian Shanxi Formation; C_{3t}: Upper Carboniferous Taiyuan Formation; C_{2b}: Middle Carboniferous Benxi Formation.

Geological Setting

The Datong Basin is located in Northern China. It is bounded by major faults to the east and south and by erosional edges in the north and west (Fig. 1). The present configuration of the basin resulted mainly from the Late Jurassic to Early Cretaceous Yanshan Orogeny. There is a major, regional unconformity separating underlying Paleozoic marine strata from Jurassic terrigenous clastic sediments. The Lower Jurassic Yongdingzhuang Formation was deposited during the earliest stage of basin infill (J_{1y} in Fig. 1). The Middle Jurassic Datong (J_{2d}) and Yungang formations (J_{2y}) form a northward, onlapping succession of strata (Fig. 1). The basin paleotopography was negligible following deposition of the Middle Jurassic Datong Formation, which has a maximum thickness of 240 m in the southern part of the basin, but decreases gradually to 50 m in the north. The most important coal-bearing strata in this part of China are of Jurassic age (Chen and Dai, 1962; Jia and Li, 1988; Liu and Li, 1996), and all of the commercial coals are produced from the Datong Formation.

The Jurassic System in the Datong Basin was dominated by fluvial, lacustrine, and lacustrine-deltaic sedimentation (Chen and Dai, 1962; Jia and Li, 1988; Liu and Li, 1996). The paleocurrent direction of the Jurassic rivers was from the north (Chen and Dai, 1962; Jia and Li, 1988; Liu and Li, 1996). The provenance of sediments is interpreted to be Precambrian

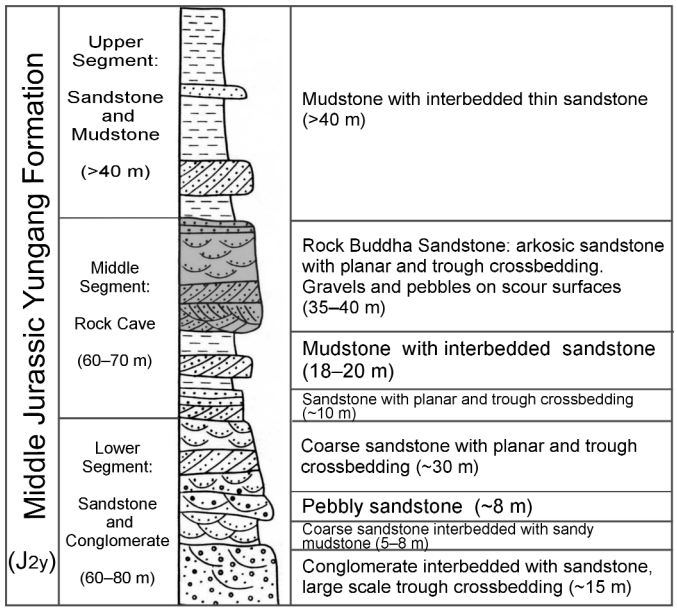

Fig. 2. Generalized lithostratigraphic chart of the Middle Jurassic Yungang Formation in the Datong Basin. The stratigraphic position of the studied outcrops is shaded.

gneiss that occurs northeast of the basin (Chen and Dai, 1962; Jia and Li, 1988; Liu and Li, 1996). The Lower Jurassic Yongdingzhuang and Middle Jurassic Datong formations were deposited predominantly by meandering rivers (Chen and Dai, 1962; Jia and Li, 1988; Liu and Li, 1996). The Middle Jurassic Yungang Formation, the focus of this investigation, consists of predominantly braided river deposits (Chen and Dai, 1962; Jia and Li, 1988; Liu and Li, 1996) (Fig. 2).

The studied outcrops of the Middle Jurassic Yungang Formation are located close to the eastern margin of the basin (Fig. 1), about 14 km west of Datong City (Shanxi Province) and 2 km east of Yungang Rock Cave, one of the most popular tourist sites in China. These outcrops are near the axis of the Yungang Syncline. The strata are nearly horizontal, with dips less than 5°. There are no faults or minor folds in these outcrops, but there are a few joints and fractures. The outcrops are divided into three sections (Fig. 1). Section A was exposed during the construction of Highway 109. The total exposure in section A is more than 500 m, with a continuous exposed section of about 350 m. Section B was cut during construction of a railway for coal transportation. Section B consists of about 150 m of continuous exposure in addition to several, shorter intervals. The strike direction of section A and B is about 110°. The vertical exposure of both sections A and B is 10 to14 m. A third section, section C, is perpendicular to sections A and B and contains shorter, discontinuous, natural exposures. Our investigation focused on section A, which was studied and measured in detail. Additional information was also gathered from sections B and C and a number of small scattered outcrops.

The depositional environment of the Yungang Formation is interpreted to be the middle-stream reaches of a proximal, sandy, braided river, based on the results of this investigation and correlation with other outcrops around section A. The fluvial deposits are elongated from north to south, corresponding to the paleocurrent direction. Towards the north, the sandstone bodies can be traced for 4 to 5 km where they are covered by the Quaternary loess. Southward, the fluvial sandstones are overlain by strata near the Jinhua Palace Coal Mine. In a section that is perpendicular to the paleocurrent direction, the maximum thickness of the exposed sandstone body is about 36 m (the basal contact is not completely exposed) and the maximum width is about 1500 m. The width to thickness ratio of the studied fluvial system is 41:7.

Research Methodology

Thirty-five vertical profiles (A1 to A35) were measured over a distance of 350 m along the section A (Figs. 3, 4). The spacing between each vertical profile is about 8 to 10 m, depending on the accessibility of the outcrop. The color and grain size of rocks, their sedimentary structures, and lithofacies were described at each profile. The geometry of sandstone bodies and their lateral changes are shown in a mosaic photograph (Fig. 3).

A total of 282 samples were collected from 35 vertical profiles (A1 to A35) along section A (Fig. 4). Due to accessibility problems, the sample density in the uppermost part of the section is much lower than in the lower part of the section (Fig. 4). All 282 samples were analyzed for porosity and permeability. In addition, 99 thin sections were made from selected samples. Grain size analyses were performed on 50 thin sections, and 30 samples were selected for clay mineral X-ray analysis.

Sedimentology

In order to establish the spatial distribution of sandstone bodies and to reconstruct the depositional history of this fluvial system, lithofacies were identified, based on petrology and sedimentary structures. These lithofacies were grouped into architectural elements. Based on the spatial distribution of lithofacies and architectural elements, the depositional history and processes that influenced the fluvial deposits were interpreted.

Lithofacies

A lithofacies is a body of rock with specific textures and petrographic characteristics. In the case of sedimentary rocks, it is based on colour, composition, fossil content, grain size and sedimentary structures (Reading, 1978; Robert and Jackson, 1987). Based on Miall's general lithofacies classification scheme (Miall, 1978a, 1978b, 1988), 17 lithofacies (Figs. 5, 6) are identified in Yungang Formation outcrops. A brief description and interpretation of each lithofacies is given in Figure 5.

Architectural Element

Various lithofacies can be grouped as "architectural elements", which are characterized by a distinctive facies assemblage, internal geometry, external form, and vertical profile (cf. Miall, 1985, 1988). The recognition of architectural elements, their characteristics and their relationships, allow an interpretation of local and regional processes of fluvial evolution in the basin (Miall, 1978a, 1978b, 1985; Allen, 1983; Yu et al., 1992). The 17 lithofacies identified in the Yungang Formation are grouped into seven architectural elements: channel fill, longitudinal bar, transverse bar, diagonal bar, abandoned channel fill, levee sediments, and overbank fines (Figs. 3, 4).

Channel Fill (CH): Gm→ St-le or St-lc→ Sm-v→ St-sn→ Sh→ M-cm

Channel fill consists mainly of medium to very coarse sandstones with trough crossbedding (including St-le, St-lc and St-sn), with minor massive sandstones (Sm-v), and massive or crudely bedded gravel (Gm) at the bases (Figs. 3, 4, 6G). These strata show a thinning-upward and fining-upward trend. Channel bases are conglomeratic (Gm) and interpreted to have been deposited by high-gradient, braided streams with great fluctuations in discharge. The lower part of the channel-fill

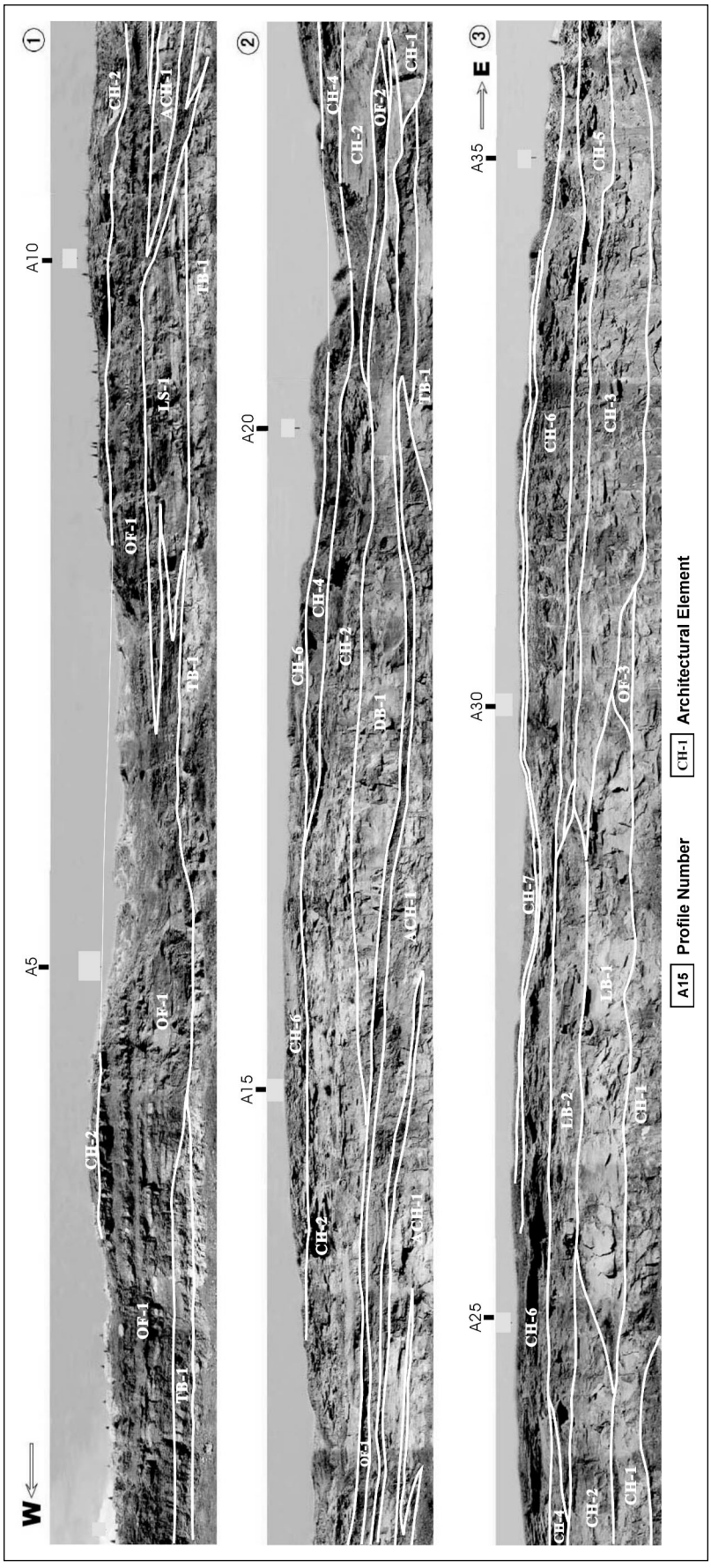

Fig. 3. A panorama view of section A of the studied outcrops. Three photographs show a continuous section from west (the upper left of the photo) to east (the lower right of the photo). The total width of the section is about 350 m and the vertical height of the section is 10–15 m. The spatial distribution of different architectural elements is highlighted.

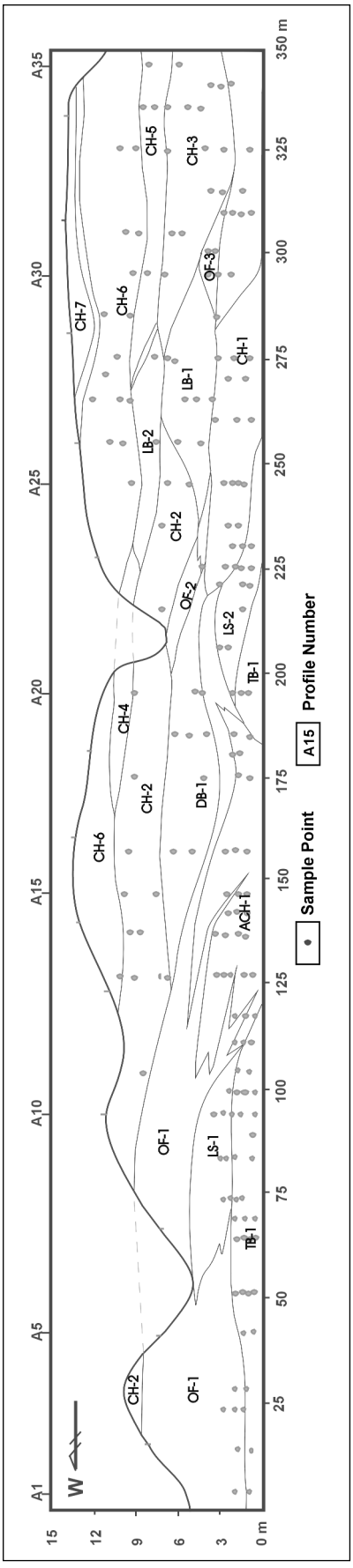

Fig. 4. Sample locations indicated on a sketch of the cross-section, based on outcrop photography (Fig. 3). The spatial distribution of different architectural elements is highlighted. Note the vertical exaggeration is about 3.5 times.

succession contains large-scale trough crossbedding (St-le and St-lc) and massive bedding (Sm-v). These sandstone bodies were deposited during the early stage of channel development when the cross-section of river channel was narrow and water level and sediment load high. Higher in the succession, sandstones with parallel or flat bedding, were deposited during late stage of channel development in wide shallow channels. Mudstones (M-cm) at the top of the fill succession formed during the last stages of channel abandonment and infill. In cross-section, channel fill sandstone bodies are lenticular or wedge-shaped with an erosional, concave base. The deposition of channel-fill sandstones occurred mainly during high-discharge events and by lateral and vertical accretion, along with channel cutting and abandonment (Sánchez-Moya et al., 1996).

Channel fills are common architectural elements in the Yungang Formation. There were seven channel-fill units identified (CH1 to CH7 in Figs. 3, 4). Channel-fill sequences are 3 to 5 m thick and occur mostly in the eastern part of section A (A23 to A35) and the upper part of the middle section (A10 to A23) (Fig. 4).

Longitudinal Bar (LB): Sp-glc → Sp-shc → Sh

Longitudinal bars are characterized by fine to coarse sandstones with planar-tabular bedding (Sp) (Fig. 6A), or horizontal lamination (Sh). From base to top, bars contain planar-tabular crossbedded sandstone with low-angle (<10°) convergent laminations (Sp-glc), overlain by sandstones with planar-tabular crossbedding and high-angle (>10°) convergent laminations (Sp-shc). These are capped by fine to coarse sandstones with horizontal laminations (Sh). In cross-section, longitudinal bars are lenticular or wedge-shaped with a flat or an erosional, concave base and a convex top (Figs. 3, 4).

Code		Depiction	Grain Size	Sedimentary Structure Description	Interpretation
Gm			massive or crudely bedded gravel	horizontal bedding, imbrication	longitudinal bars, lag deposits, sieve deposits
Sp	Sp-glc		sand, fine to medium coarse may be pebbly	grouped planar-tabular crossbeds with low-angle (<10°) convergence laminations	diagonal bar
	Sp-ghb		sand, medium to very coarse may be pebbly	grouped planar-tabular crossbeds	transverse bar
	Sp-shc		sand, medium to very coarse may be pebbly	solitary planar crossbeds	longitudinal bar
St	St-le		sand, medium to very coarse may be pebbly	Solitary or grouped large bed sets (thickness >50cm) trough crossbeds with eccentric laminations	channel fills
	St-lc		sand, medium to very coarse may be pebbly	solitary or grouped large bed sets (thickness >50cm) trough crossbeds with concentric laminations	channel fills
	St-sn		sand, very fine to coarse	solitary or grouped small bed sets (thickness <50cm) trough crossbeds	small dunes
Sm	Sm-u		sand, very fine to coarse	massive with uniform grain size	abandoned channel fills
	Sm-v		sand, medium to very coarse may be pebbly	massive with various grain size	channel fills, lag deposits
Sr			sand, very fine to coarse	ripple crossiamination	current ripples
Sh			sand, very fine to coarse	horizontal lamination parting or streaming lineation	planar bed flow
Fh			silt, mud	horizontal lamination	overbank or waning flood
Fr			silt, mud	small ripple crosslamination	levee,current ripples
Fm			silt, mud	massive, desiccation cracks	overbank or drape deposits
M	M-cms		mud, silt to sand, motley	massive, desiccation cracks	overbank or backswamp deposits
	M-dh		mud, dark	horizontal lamination, shale	backswamp pond deposits
	M-cm		mud, motley (colour)	massive, desiccation cracks	overbank or drape deposits

Fig. 5. Summary of lithofacies and characteristics of Jurassic fluvial deposits, Yungang Formation outcrops, northern China. The classification scheme is based on Miall (1978b, 1988).

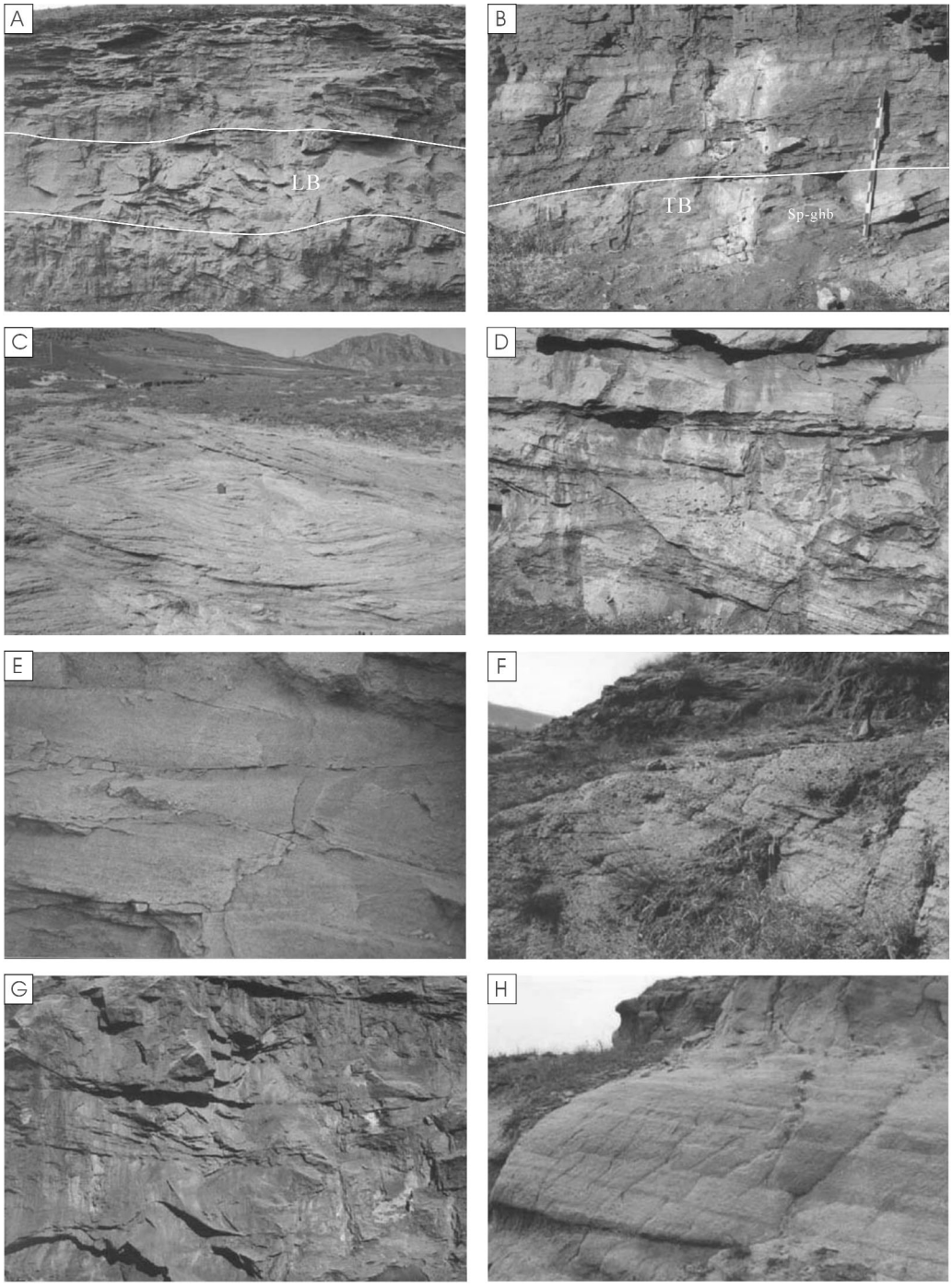

Fig. 6. Field photograph showing lithofacies and architectural elements in the braided fluvial deposits at Yungang (see Fig. 5 for the lithofacies code). **A**) A longitudinal bar (LB) with solitary planar crossbedding of high-angle convergence laminations (lithofacies Sp-shc); **B**) A transverse bar (TB) with high-angle planar-tabular crossbeds (lithofacies Sp-ghb); **C** and **D**) Trough crossbedding with large bed sets (lithofacies St-le); **E**) Trough crossbedding with small bed sets (lithofacies St-sn); **F**) Trough crossbedding with large, concentric bed sets (lithofacies St-lc); **G**) Minor channel fill with massive bedding and uniform grain size; **H**) Horizontal bedding (lithofacies Sh).

Scour surfaces with gravel and muddy clasts are common at the base. Longitudinal bars occur only in the middle part of the eastern section (e.g. LB-1 and LB-2 in Figs. 3 and 4) and are interpreted as downstream accretion bedforms (cf. Miall, 1988).

Transverse Bar (TB): St → Sp-ghb → Sh

In the Yungang Formation outcrops, transverse bars are composed mainly of planar-tabular crossbedded sandstones (Sp-ghb) and trough crossbedded sandstones (St) (Figs. 3, 4, 6B). In the lower part of the transverse bar, there are fine to coarse sandstones with small trough crossbeds (St-sn), which pass upward to planar-tabular crossbeds (Sp-ghb) (Fig. 6B). Tabular beds are 0.5 to 2.5 m thick and typically extend several tens of metres, laterally. Locally, fine to coarse sandstones with horizontal lamination (Sh) occur at the top of transverse bars. In a cross-section, transverse bars have a flat or concave-up base and a gentle-convex top (Fig. 4). Reactivation surfaces are common, suggesting that deposition took place as episodic, discontinuous stream discharge. Transverse bars have been reported as a common element in braided streams dominated by vertical accretion (e.g. Smith, 1971; Cant and Walker, 1978; Miall, 1978a; Crowley, 1983; Ramos et al., 1986; Rust and Jones, 1987; Bristow, 1993; Sánchez-Moya, 1996).

Diagonal Bar (DB): Sm-v→ Sp-glc→ St-sn

The base of the diagonal bars is composed of massive sandstones with variable grain size (Sm-v). The main lithofacies, however, consists of sandstones with planar-tabular crossbedding and low-angle (<10°) convergent laminations (Sp-glc). Locally, laminations are sigmoidal, suggesting lateral migration and lateral accretion of diagonal bars (Allen, 1983). Diagonal bars are characterized by fining-upward successions with a concave base and flat top (Fig. 4). In outcrop, only one diagonal bar was identified in the middle part of the section (DB-1 in Figs. 3 and 4), which is interpreted as a smaller channel in section A.

Abandoned Channels (ACH): Sm ←→ Sh, Fm ←→ M-dh

Abandoned channels are characterized by massive sandstone (Sm) and fine sandstone with horizontal laminations (Sh). Locally, they may also contain massive siltstone (Fm) and dark mudstone with horizontal laminations (M-dh). Desiccation cracks occur in the mudstone facies. One abandoned channel was recognized in the middle part of section A (Figs. 3, 4), and it consists of multiple, wedge-shaped, thin sandstone bodies interbedded with thick mudstones. Single sandstone layers are 0.3 to 1.5 m thick.

Levee Sediments (LS): Sm-u ←→ Fr → Fm, Fh → M-dh

Levee sediments are composed of medium to fine grained, wedge-shaped, massive sandstones interbedded with massive mudstones. Individual sandstone beds are 0.3 to 1 m thick; grain size and thickness of these sandstones decrease away from the channel. The main sedimentary structures in the levee mudstones are horizontal bedding and ripple cross-lamination. Levee sediments always occur at the flanks of abandoned channels, and their contact with overbank fines is gradational. Two levee sediment bodies were recognized in section A (Figs. 3, 4): one in the eastern part of the section (A5 to A10) and the other between profiles A20 and A25.

Overbank Fines (OF): Sm, Sh, Sr ←→ Fm ←→ M

Overbank fines consist of mudstones (M) and silty mudstones (Fm) with thin sandstone lenses (Sm, Sh, or Sr). Individual sandstone interbeds are 1.5 to 3.0 m thick and 20 to 50 m wide. These sandstones are lenticular in shape and have a concave base and a flat or convex top. Some of these sandstone lenses display a crude, coarsening-upward trend. The lateral extension of overbank fines is over 150 m. In section A, overbank fines occur mostly in the west part of the section between profiles A1 to A15 and thin dramatically towards the east (Figs. 3, 4). The cumulative thickness of the overbank fines is about 7 m (Figs. 3, 4).

Depositional History

Sandstone bodies occur as linear bands extending from north to south. In cross-section, these sandstone bodies are lenticular with a concave base and flat top (Figs. 3, 4). Frequent channel switching resulted in channel stacking. Within the sandstone complex,there are some muddy intercalations (Figs. 3, 4), but they are very thin and of limited lateral extent. Overbank floodplain fines bound channel complexes (Figs. 3, 4). The sandy, braided river developed in three stages: from active, to abandoned, and then to reactivated. These stages reflect channel switching of a fluvial system with variable discharge.

Early active stage: During an early active stage, sandstone bodies of a channel complex (e.g. TB-1) were deposited (Figs. 3, 4). The top part of TB-1 occurs in the lower western (between A1 to A10) and lower middle (A20) parts of section A. The exposed part of TB-1 is about 200 m wide.

Abandonment stage: The sandy, braided river was abandoned after deposition of TB-1, probably due to upstream channel avulsion. During this period, overbank fines were deposited, mainly in the western part of section A (OF-1 from A1 to A15) (Figs. 3, 4). However, small patches of overbank fines also occur in the east (OF-3 at A30) and central (OF-2 between A20 and A25) areas (Figs. 3, 4). Based on correlation with other outcrops, the projected lateral extension in section A is over 1500 m. Although the main channel was abandoned during this period, some small channels probably still existed, as indicated by sandstone lenses interbedded with overbank fines.

Reactivation stage: This stage is divided into 3 phases: channel incision, channel filling, and channel waning. During the early phase, strong incision is indicated by a concave, erosional surface. In section A, three incision steps are interpreted. During early filling, the water depth and sediment load were high, because the channel was relatively narrow. The deposi-

tional process during this phase was dominated by downstream and vertical accretion, resulting in large-scale trough crossbedding (e.g. CH-1 in Figs. 3 and 4). Later, the channel became wider (e.g. CH-2, CH-3, CH-4, CH-5, in Figs. 3 and 4) and water depth shallower as the channel began to bifurcate. The depositional processes changed to vertical and lateral accretion, forming longitudinal bars and diagonal bars with large-scale planar or tubular crossbedding. In the final phase of the channel infill, sandstone bodies were formed by small- to medium-scale bedforms (e.g. CH-6 in Fig. 4). During the channel waning phase, fine sediments were deposited.

Reservoir Characterization

In order to characterize the reservoir properties and to understand heterogeneities of reservoirs in this fluvial system, we have examined the petrography of sandstones, measured porosity and permeability of seven architectural elements, and mapped spatial variation of porosity and permeability along cross-section A.

Petrology of Reservoirs

The sandstones in the fluvial system in section A are arkosic and lithic-arkosic. The following are some of the key characteristics of these sandstones, based on examination.

High matrix content: The matrix content is more than 15% in sandstones sampled from the eastern and middle part of section A. However, a few samples from small, lenticular sandstone bodies in the western part of the section have less than 15% matrix.

Low compositional maturity: The abundance of quartz grains in the sandstones ranges from 33 to 66%, feldspar grains from 20 to 36%, and lithic grains from 6 to 39%. Most samples from channels in the east and middle segments have less than 50% quartz grains but more than 20% lithic fragments. The dominant lithology of sandstones in these outcrops is, therefore, feldspar lithic graywacke or lithic feldspar graywacke.

Low textural maturity: Grain size in most of the samples is bimodal with poor or moderate sorting. The grain size ranges from –0.19 to 2.1ø (average from 0.05 to 2.1ø) based on an analysis of 50 thin sections. The shape of most detrital grains is subangular to subrounded, although some angular grains also occur.

Variety of cement: Cement identified in thin sections includes calcite, siderite, kaolinite, and illite. Calcite cement occurs as a thin film around grains or as blocky cements in pores. Locally, calcite also replaced feldspar or quartz grains. Kaolinite and illite are cryptocrystalline, or occur as microcrystalline flakes. Siliceous cement is rare and occurs as quartz overgrowths.

The low compositional and textural maturity suggests that these sediments were deposited proximal to their source. The high content of metamorphic fragments indicates a metamorphic source area at the northern edge of the basin.

Petrophysics of Architectural Elements

A total of 282 samples from seven architectural elements in section A were analyzed for porosity and permeability in order to characterize the petrophysical property of reservoirs in this fluvial system. The porosity and permeability data obtained in this study indicate that 1) different architectural elements have different porosity and permeability and 2) there is also internal variation in petrophysical properties, even within a single architectural element. The heterogeneity of reservoirs in the studied fluvial system is related to variation of the petrophysical properties amongst different architectural elements, as well as within a single architectural element.

The porosity and permeability of individual architectural elements were plotted in Figure 7. The slopes of the best-fit lines indicate the sensitivity of permeability responses to porosity change. A steep slope in Figure 7 indicates that a small change of porosity would result in a relatively large change in permeability. A gentle slope, on the other hand, indicates that permeability and porosity are not easily related. Among seven architectural elements from Yungang Formation, the slopes of the best-fit lines for channel fills (CH) and various sandstone bars (LB, TB, and DB) are steeper than levee sediments (LS) and overbank fines (OF) (Fig. 7). Therefore, when porosity increases, the permeability in these channels fills and sandstone bars increases more dramatically than those of levee sediments and/or overbank fines.

Table 1. Petrophysical statistics of the architectural elements of the Yungang Formation outcrops.

Code	No. of samples	Porosity (%)				Permeability (md)			
		Min	Max	Average	SD	Min	Max	Average	SD
CH	135	5.7	16.6	9.7	1.30	0.02	7.76	0.53	0.44
LB	35	9	13.3	10.4	1.05	0.12	10.8	1.15	1.38
TB	14	3	10.4	6.9	1.00	0.01	2.16	0.22	0.26
DB	24	6	11.2	8.3	1.05	0.03	0.7	0.22	0.18
ACHH	43	2.4	9.7	5.8	1.32	0.01	0.92	0.08	0.09
LS	23	3.3	10.9	6.7	1.32	0.02	0.08	0.04	0.01
OF	10	3	9.9	7.6	1.73	0.04	0.2	0.10	0.04

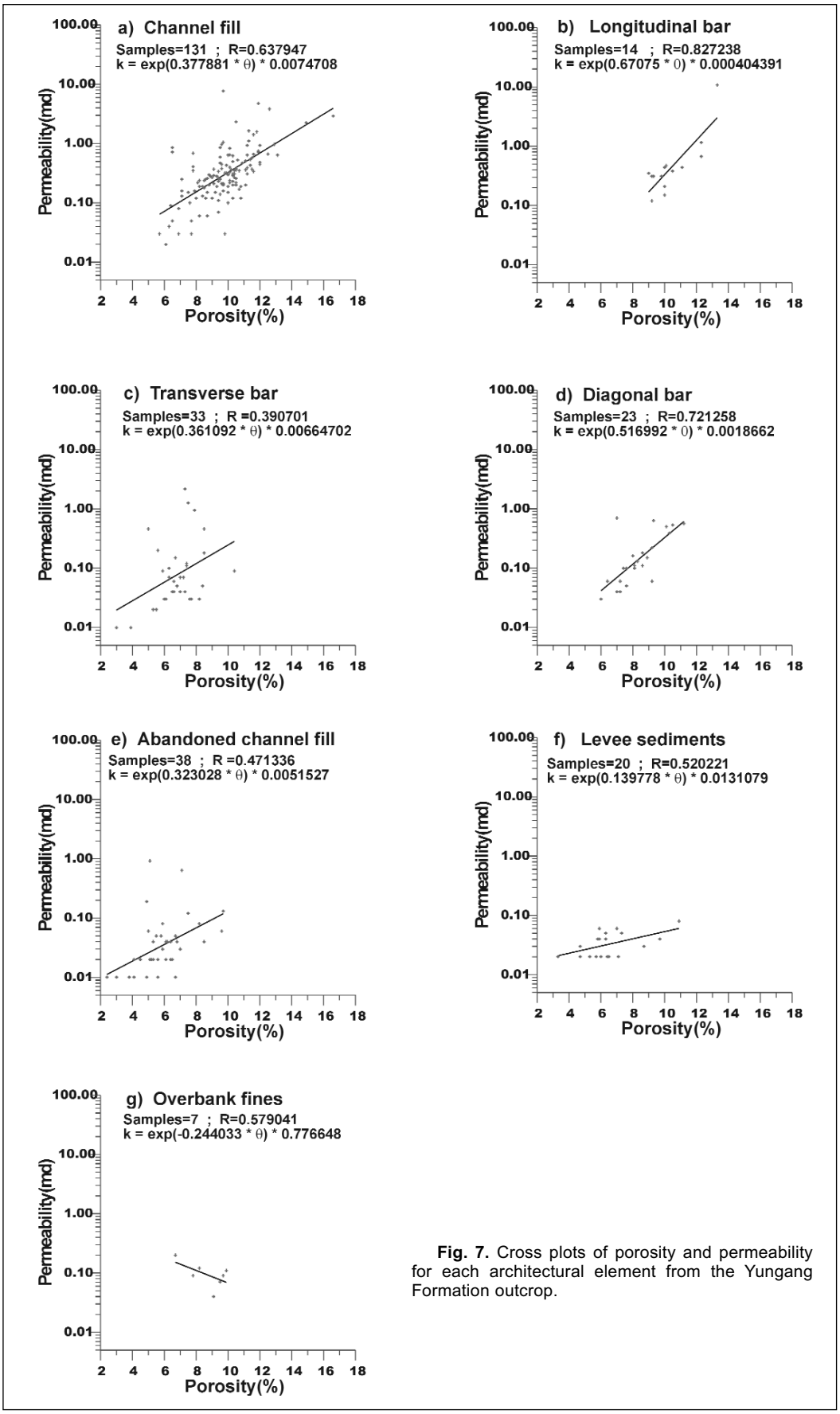

Fig. 7. Cross plots of porosity and permeability for each architectural element from the Yungang Formation outcrop.

Statistical analyses of porosity and permeability data are summarized in Table 1. The average values of porosity and permeability for each architectural element are presented in Figure 8. The results show that longitudinal bars (LB) have the highest porosity and permeability, averaging 10.4% and 1.2 md, respectively (Table 1; Fig. 8). Abandoned channels (ACH) and levee sediments (LS) have the lowest porosity and permeability, with average porosity ranging from 5.8% to 6.7% and permeability from 0.08 to 0.04 md (Table 1; Fig. 8).

The spatial variation of porosity and permeability of channel fills and different bars is shown in Figure 9. The porosity and permeability in the middle section of the sandstone bodies are generally higher than those from the top and bottom sections (Fig. 9). Areas of higher porosity and permeability generally correspond to spatial distribution of longitudinal bar (LB) and channel fill (CH), suggesting that reservoir heterogeneity is related to the spatial distribution of architectural elements.

The internal, spatial distribution of porosity and permeability within a single architectural element is also variable (Fig. 10) due to lithological and sedimentary structure variability. The internal distribution of porosity and permeability in the diagonal bar generally decreases upward in a direction orthogonal to laminations. This decrease is apparently related to the spatial distribution of lithofacies and sedimentary structures. The porosity and permeability vary in transverse bars as a result of interbeds. The porosity and permeability distribution in longitudinal bars is relatively uniform with a slight decrease at the bar tops and margins (Fig. 10). The porosity and permeability are high in the central part of the channel fills and decrease towards the margins. Channel fills are sandier in the centre and muddy pebbles and shale detritus often occur along their margins.

Application To Oil Production In Eastern China

The data and information gathered from this outcrop study will provide a better understanding of lithofacies distribution, sandstone body geometry, and reservoir heterogeneity of the braided sandstones of the Meso-Cenozoic basins in eastern China, including Gudao and Shengtuo oilfields in the Jiyang Basin; Dagang oilfield in the Huanghua Basin; Penglai 19-3 oilfield in the Bohai Basin (Wu and Xue, 1992); and Daqing oilfield (e.g. the Saertu-Putaohua pools) in the Songliao Basin (Wang, 1996). In these oilfields, the hydrocarbon production is hampered by the lack of understanding of reservoir geometry and heterogeneity due to limited well log information and core samples.

The preliminary analyses indicate that the lithofacies, architectural elements, and sandstone geometry of our studied outcrops are similar to the reservoirs of these oilfields (e.g. Gudao and Shengtuo oilfields in the Jiyang Basin). If the data set obtained from this outcrop study can be integrated with the log analyses and core examination, it will be possible to better characterize architectural elements and to predict geometry and heterogeneity of these sandstone reservoirs. The appropriate production strategy could be designed and implemented to maximize oil recovery in these fields.

Conclusions

Seventeen lithofacies are identified in outcrops of Middle Jurassic braided fluvial strata in the Datong Basin, based on petrology and sedimentary structures. These lithofacies are grouped into seven architectural elements. Fluvial strata were deposited in three stages: active, abandonment, and reactivation, reflecting channel switching and variable discharge of the fluvial system.

The channel fills and fluvial bars consist of arkosic or lithic-arkosic sandstones, with high matrix content, low compositional and textural maturity, and a variety of cements. Petrophysical analysis indicates that different architectural elements have different porosity and permeability; and even within a single architectural element there is internal variation in petrophysical properties. Sandstones from longitudinal bars and channel fills have the highest porosity and permeability, while abandoned channels and levee sediments have the lowest. In 350 m of continuous outcrop, the porosity and permeability in the middle part of the sandstone bodies is generally higher than that of the top and bottom. Reservoir heterogeneity in this fluvial system is, therefore, related to the spatial distribution of different architec-

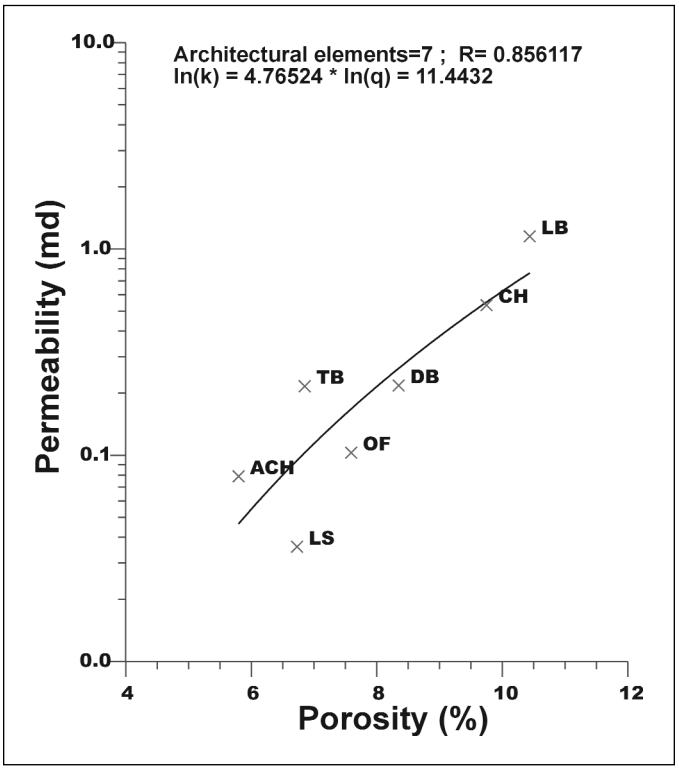

Fig. 8. A cross plot of average porosity and permeability for different architectural elements of Yungang Formation outcrop. It shows architectural element LB as exhibiting the highest porosity and permeability, whereas LS has the lowest porosity and permeability. CH=channel fill, LB=longitudinal bar, DB=diagonal bar, TB=transverse bar, OF=overbank fines, AC=abandoned channel fill, LS=levee sediments.

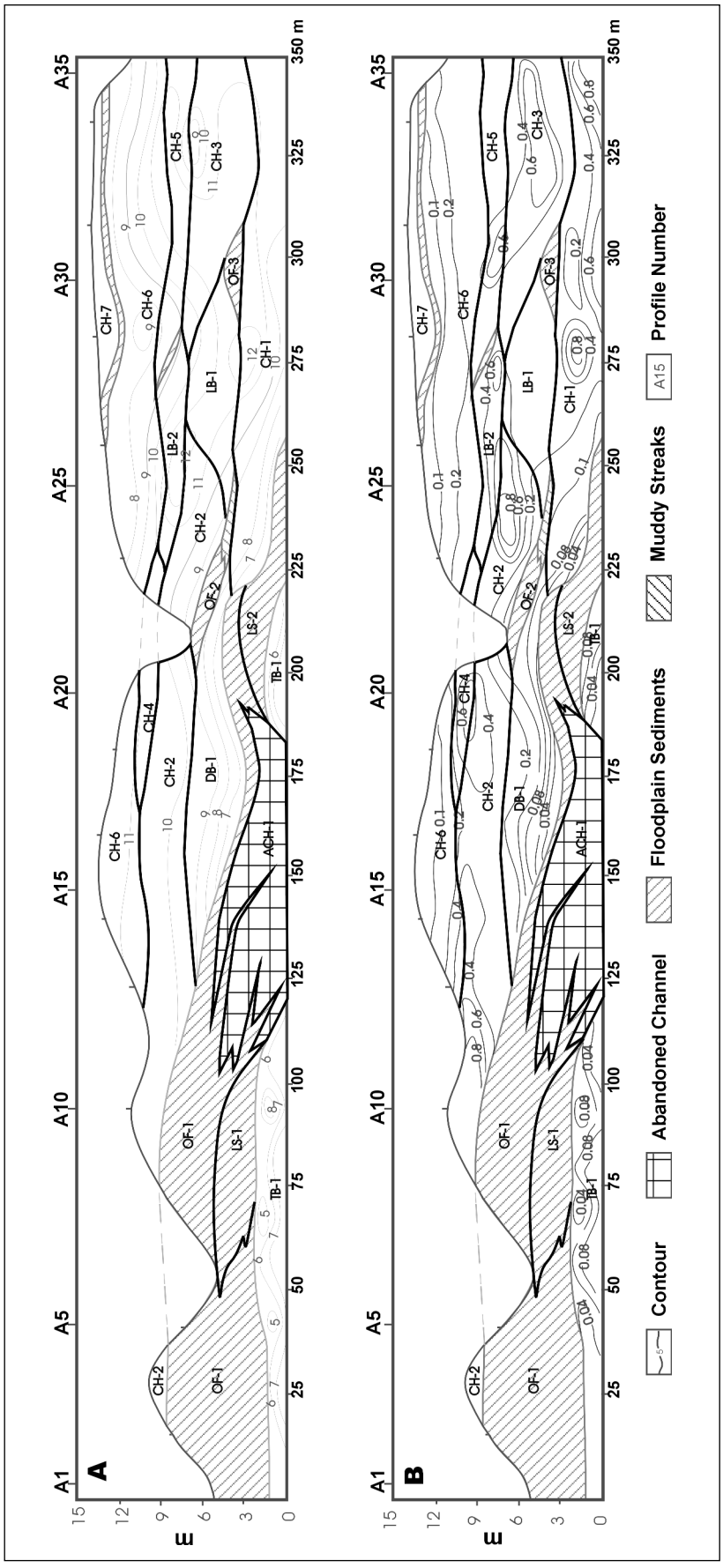

Fig. 9. The contour of porosity (**A**) and permeability (**B**) for the braided-fluvial system of Yungang Formation outcrop. The spatial distribution of different architectural elements is highlighted in the background.

Architectural Elements	Lithofacie Assem-blage	Depositional Process	Geometry and Internal Structure	Original Data and Contour of Porosity (%)	Original Data and Contour of Permeability (md)
Diagonal Bar	Sp-glc Sm-v	Lateral and Vertical Accretion	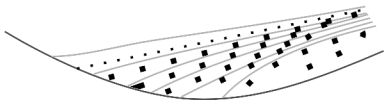	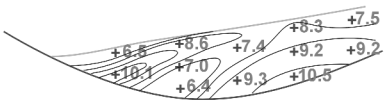	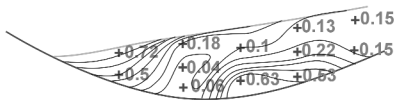
Transverse Bar	Sh Sp-ghb	Vertical Accretion	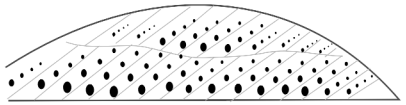	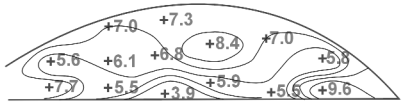	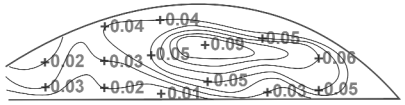
Longitudinal Bar	Sh Sp-shc	Down-stream Accretion	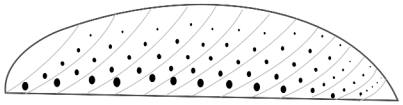	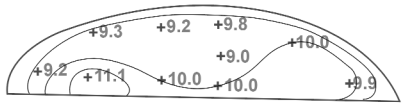	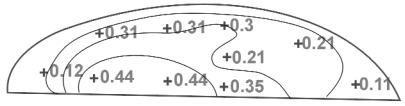
Channel Filling	M-cms St-sn St-lc or Sp or Sm-a	Vertical accretion and channel fills	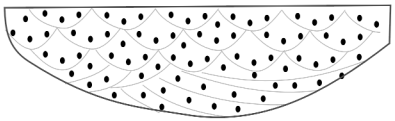	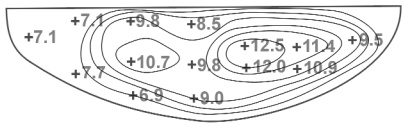	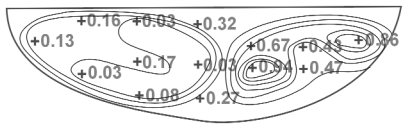

Fig. 10. The internal reservoir characteristics of sandstone bars and channel fills.

tural elements and variation of petrophysical properties within individual architectural elements.

This outcrop study provides an analog for a better understanding of the architecture and heterogeneity of hydrocarbon reservoirs in a similar geologic setting in eastern China where a significant number of petroleum reservoirs are fluvial-deltaic sandstones deposited in the Cenozoic-Mesozoic terrestrial basins.

Acknowledgments

We acknowledge financial support for this study from the Research Institute of Petroleum Exploration and Development of PetroChina; the Ministry of Education of China (Project 211), and the Ministry of Land and Resources of China. Part of the work was finished while the senior author was a visiting professor at the University of Regina. We appreciate discussions with Prof. Yinan Qiu, Longxing Mu, and Dr. Ailin Jia and field assistance by Dr. Liang Chen and Shiyan Huang. Constructive comments by Drs. Peter McCabe, John Robinson, and Caroline Williams have substantially improved this manuscript.

References

Allen, J.R.L. 1983. Studies in fluviatile sedimentation: bars, bar-complexes and sandstone sheets (low-sinuosity braided streams) in Brownstones (L. Devonian), Welsh border. Sedimentary Geology, v. 33, p. 237-293.

Bristow, C.S. 1993. Sedimentary structure exposed in bar tops in the Brahmaputra River, Bangladesh. In: Braided Rivers. J.L. Best and C.S. Bristow (eds.). Geological Society of London, Special Publication 17, p. 277-289.

Cant, D.J. and Walker, R.G. 1978. Fluvial processes and facies sequences in the sandy braided South Saskatchewan River, Canada. Sedimentology, v. 25, p. 625-648.

Chen, Y. and Dai, D. 1962. The facies of Jurassic System in Datong district, Shanxi Province, China. Geology Bulletin, v. 42, no. 3 (in Chinese).

Crowley, K.D. 1983. Large-scale bed configuration (macroforms), Platte River Basin, Colorado and Nebraska: Primary structures and formative processes. Geological Society of America Bulletin, v. 94, p. 117-133.

Jia, B. and Li, T. 1988. The depositional environments of the Datong coalfield. Science Press, p. 85-92 (in Chinese).

Liu, S. and Li, J. 1996. The geology summary of Jurassic coal-field in Datong mining district. Datong Mining Bureau, Publication 13, p. 93-105 (in Chinese).

Miall, A.D. 1978a. Fluvial sedimentology: an historical review. In: Fluvial sedimentology. A.D. Miall (ed.). Canadian Society of Petroleum Geologists, Memoir 5, p. 1-47.

_____ 1978b. Facies types and vertical profile models in braided river deposits: a summary. In: Fluvial sedimentology. A.D. Miall (ed.). Canadian Society of Petroleum Geologists, Memoir 5, p. 597-604.

_____ 1985. Architectural-element analysis: a new method of facies analysis applied to fluvial deposits. Earth Science Reviews, v. 22, p. 261-308.

_____ 1988. Reservoir heterogeneities in fluvial sandstones: lessons from outcrop studies. American Association of Petroleum Geologists Bulletin, v. 72, p. 682-697.

Ramos, A., Sopeña, A. and Pérez-Arlucea, M. 1986. Evolution of Buntsandstein fluvial sedimentation in the northwest Iberian ranges (Central Spain). Journal of Sedimentary Petrology, v. 56, p. 862-875.

Reading, H.G. 1978. Sedimentary environments and facies. Blackwell Scientific Publications, 615 p.

Robert, L.B. and Jackson, J.A. 1987. Glossary of Geology. American Geological Institute, Alexandria, Virginia, 383 p.

Rust, B.R. and Jones, B.G. 1987. The Hawkesbury Sandstone south of Sydney, Australia: Triassic analogue for deposit of a large, braided river. Journal of Sedimentary Petrology, v. 57, p. 222-233.

Sánchez-Moya, Y., Sopeña, A. and Ramos, A. 1996. Infill architecture of a nonmarine half-graben Triassic Basin (Central Spain). Journal of Sedimentary Research, v. 66, p. 122-1136.

Smith, N.D. 1971. Transverse bar and braiding in the lower Platte River, Nebraska. Geological Society of America Bulletin, v. 82, p. 3407-3420.

Yu, X, Wang, D. and Zheng, J. 1992. Lithofacies association types or sequences and depositional system of Permian sandstones in North China. Acta Sedimentologica Sinica, v. 10, no. 3, p. 27-35 (in Chinese).

_____, _____ and Sun, Z. 1994. 3-D Extension Models Of Braided Deltaic Sandbody in Terrestrial Facies – An Observation on Deposition of Modern Deltas in Daihai Lake, Inner Mongolia. Acta Petrolei Sinica, v. 15, p. 26-37 (in Chinese).

Qiu, Y. 1992. The reservoir sedimentology advances of terrestrial clastic rocks, China. Acta Sedimentologica Sinica, v. 10, p. 16-24 (in Chinese).

Wang. T. 1996. The geology of oil and gas accumulation of rift basins in east China. Petroleum Industry Press, Beijing, p. 78-79 (in Chinese).

Wu, C. and Xue, S. 1992. The sedimentology of petroliferous basins in China. Petroleum Industry Press, Beijing, p. 28 (in Chinese).

Manuscript received: April 17, 2001

Revised manuscript accepted: September 17, 2001